Discovery of 7-azaindole derivatives as potent Orai inhibitors showing efficacy in a preclinical model of asthma

ARTICLE *in* BIOORGANIC & MEDICINAL CHEMISTRY LETTERS · FEBRUARY 2015

Impact Factor: 2.42 · DOI: 10.1016/j.bmcl.2015.01.063

12 AUTHORS, INCLUDING:

Sonia Sentellas

Almirall

27 PUBLICATIONS **442** CITATIONS

SEE PROFILE

Irene Jover

Almirall

3 PUBLICATIONS **4** CITATIONS

SEE PROFILE

Montse Miralpeix

Almirall

83 PUBLICATIONS **2,561** CITATIONS

SEE PROFILE

Bernat Vidal

Almirall

39 PUBLICATIONS **501** CITATIONS

SEE PROFILE

Bioorganic & Medicinal Chemistry Letters 25 (2015) 1217–1222

Contents lists available at ScienceDirect

Bioorganic & Medicinal Chemistry Letters

journal homepage: www.elsevier.com/locate/bmcl

Discovery of 7-azaindole derivatives as potent Orai inhibitors showing efficacy in a preclinical model of asthma

Cristina Esteve, Jacob González, Sílvia Gual, Laura Vidal, Soledad Alzina, Sonia Sentellas, Irene Jover, Raquel Horrillo, Jorge De Alba, Montserrat Miralpeix, Gema Tarrasón, Bernat Vidal *

Almirall Research Center, Almirall, Ctra. Laureà Miró 408, E-08980 St. Feliu de Llobregat, Barcelona, Spain

ARTICLE INFO

Article history:
Received 10 November 2014
Revised 26 January 2015
Accepted 27 January 2015
Available online 4 February 2015

Keywords:
Orai inhibitors
IL-2 inhibitors
LAD2
CRAC channel
OVA model

ABSTRACT

Synthesis and SAR of a series of 7-azaindoles as Orai channel inhibitors showing good potency inhibiting IL-2 production in Jurkat cells is described. Compound **14d** displaying best pharmacokinetic properties was further characterized in a model of allergen induced asthma showing inhibition in the number of eosinophils in BALF. High lipophilicity remains as one of the main challenges for this class of compounds.

The regulation of intracellular calcium is a key element in the transduction of signals into and within cells. Cellular responses to growth factors, neurotransmitters, hormones and other signal molecules are initiated through calcium-dependent processes. Virtually all cell types depend upon the generation of cytoplasmic calcium signals to regulate cell function or to trigger specific responses. Cytosolic calcium signals control a wide array of cellular functions ranging from short-term responses such as contraction and secretion to longer-term regulation of cell growth and proliferation. These signals involve combination of calcium release from intracellular stores such as the endoplasmic reticulum (ER), and influx of calcium across the plasma membrane.[1]

In immune cells the molecular mechanisms of calcium signaling are especially well characterized. Cell activation through immunoreceptor engagement induces a rise in cytosolic calcium levels mainly through a selective channel-based process known as Store-operated calcium entry (SOCE). Calcium release-activated calcium (CRAC) channels are a type of SOC channels present in B and T-lymphocytes, NK cells, macrophages, DC and mast cells among the immune cells. CRAC channels are characterized by an extremely high ion selectivity for Ca^{2+} and a low conductance, and are activated through a Ca^{2+} sensor protein in the ER called stromal interaction molecule (STIM) that bind to Orai, the pore forming unit of the CRAC channel in the plasma membrane. Upon antigen binding to the T-cell receptor, the activation of phospholipase C (PLCγ) generates the lipid metabolite InsP3, which promotes the release of Ca^{2+} from the ER stores. STIM proteins sense the calcium depletion in the ER, oligomerize and redistribute into discrete puncta located in junctional ER sites in close proximity to the plasma membrane. STIM proteins directly interact with Orai1 in the plasma membrane opening the CRAC channel and allowing a sustained calcium entry across the plasma membrane.[2–4] Such a prolonged intracellular calcium increase activates short term processes such as degranulation, and long term processes involving gene transcription through NFAT to produce lipid mediators, several cytokines Th1, Th2, and Th17, matrix metalloproteinases, all of which participate in the pathogenesis of autoimmune and inflammation-based diseases.

Based on this, Orai1 inhibition is expected to exert broad anti-inflammatory activity by suppressing T cell activation and mast cell degranulation, and may have therapeutic potential in all disease stage of respiratory diseases such as asthma.[5,6]

We envisaged the exploration of 7-azaindoles as an area of further optimization around Orai inhibitors as bicyclic isosteric replacements of the arylcarboxamide motif. This could provide a new entry point to explore SAR towards compounds with increased polarity versus highly lipophilic reference compounds **1** and **2** (measured $logD_{7.4}$: 4.4 and 3.5, respectively) (Fig. 1).

Our initial SAR was based on exploring substitutions in position 2 of the 7-azaindole core ring keeping the 1-methyl-3-(trifluoromethyl)-1*H*-pyrazol-5-yl group in position 5 as this is a motif

* Corresponding author. Tel.: +34 93 291 3996; fax: +34 93 312 8615.
E-mail address: bernat.vidal@almirall.com (B. Vidal).

http://dx.doi.org/10.1016/j.bmcl.2015.01.063
0960-894X/

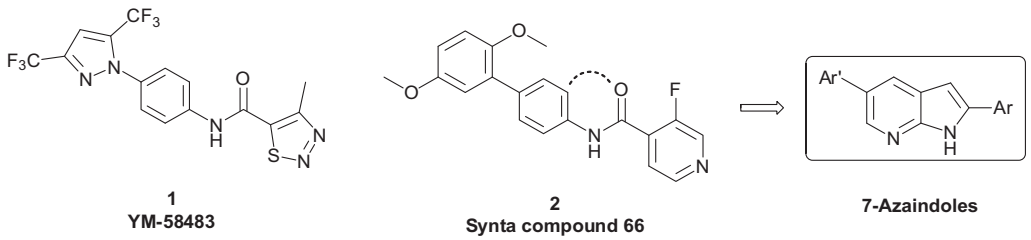

Figure 1. Orai channel inhibitors.

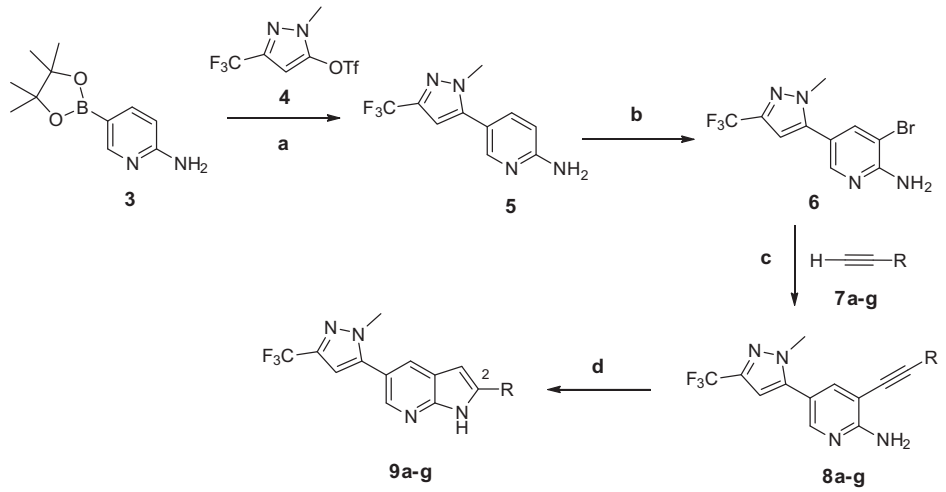

Scheme 1. Reagents and conditions: (a) $PdCl_2$dppf.DCM, Cs_2CO_3, dioxane–water, 110 °C, 35%; (b) NBS, acetonitrile, 0 °C to rt, 2 h, 30%; (c) CuI, $(Ph_3P)_2PdCl_2$, Et_3N, THF, 90 °C, 4 h, 68–97%; (d) for **9a**–**c**: *t*-BuOK, *N*-methylpyrrolidinone, rt, 20–67%; for **9d**–**g**; (i) 2,2,2-trifluoroacetic anhydride, dioxane, rt, 1 h, (ii) Et_3N, DMF, 120 °C, 20 h, 25–30% (two steps).

reported to be well tolerated in similar series of Orai inhibitors.[7] Thus, a synthesis was devised in order to access molecules containing different substituents in position 2 of the 7-azaindazole core (Scheme 1). Suzuki-type coupling reaction of commercially available boronate **3** with the triflate of 1-methyl-3-(trifluoromethyl)-1*H*-pyrazole **4** provided aminopyridine **5**. Bromination followed by Sonogashira type coupling with a diverse set of alkynes **7a**–**g** provided key intermediates **8a**–**g** that were converted into compounds **9a**–**g** using a base-mediated indolization reaction in *t*-BuOK at room temperature or using a sequential trifluoroacetylation- cyclization sequence.[8,9]

The synthesis of 7-azaindole derivatives **14a**–**n** is described in Scheme 2. Chemoselective Sonogashira type coupling of 5-bromo-3-iodopyridin-2-amine (**10**) with 1-chloro-2-ethynyl-3-fluorobenzene (**11**) provided compound **12**. Base mediated cyclization with *t*-BuOK/NMP afforded intermediate **13**. Suzuki type coupling of intermediate **13** with the corresponding boronic acids or boronates of R^1 provided compounds **14a**–**n**.

Compounds **9a**–**g** were tested in a fluorescence-based assay of store operated calcium entry in Jurkat cells.[10] Furthermore, their ability to inhibit NFAT induced transcription was monitored through the evaluation of IL-2 released from Jurkat T cells.[11] A first round of optimization with a limited set of substitutions in position 2 of the azaindole core (Table 1) led us to the 2,6-disubstituted phenyl group as providing best potency in both assays. 2-Chloro-6-fluorophenyl substituted compound **9b** was a good starting point with an IC_{50} of 66 nM in the calcium assay and an IC_{50} of 23 nM in the IL-2 assay. When slightly polar groups (**9f**) or a benzyl group (**9g**) were introduced, the activity inhibiting calcium influx and IL-2 dropped dramatically. For compounds **9a**–**e** we observed a good correlation between the activity in the calcium and the IL-2 assays.

We then explored replacement of the 3-(trifluoromethyl)-1*H*-pyrazol-5-yl group in position 5 with disubstituted aryl and heteroaryl groups as well as bicyclic derivatives, maintaining the 2-chloro-6-fluorophenyl substitution in position 2 (Table 2) as is was the best substitution providing additivity based on internal

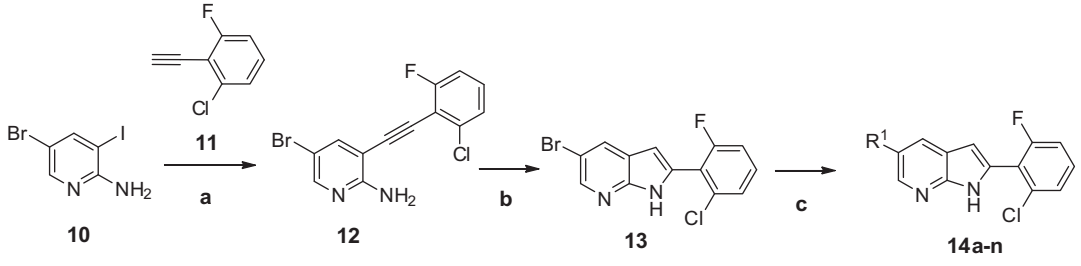

Scheme 2. Reagents and conditions: (a) CuI, $PdCl_2(PPh_3)_2$, Et_3N, DMF, 110 °C, 82%; (b) *t*-BuOK, *N*-methylpyrrolidinone, rt, 34%. (c) R^1-$B(OH)_2$ or R^1-pinacolboronate, $PdCl_2$dppf.DCM, Na_2CO_3, EtOH-toluene, 90 °C, 70–85%.

Table 1
Jurkat Ca^{2+} and IL-2 secretion inhibition of selected 7-azaindole derivatives[a]

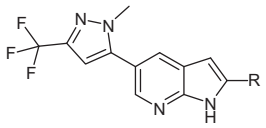

Compound	R	Jurkat calcium inhibition IC_{50} (nM)	Jurkat IL-2 secretion inhibition IC_{50} (nM)	*c*Log*P*	LipE[b]
1 YM	—	75 ± 40	10 ± 1	4.1	3.0
2 Synta	—	82 ± 24	10 ± 2	3.3	3.8
9a	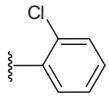	160 ± 17	260 ± 1	4.6	2.2
9b	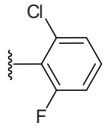	66 ± 39	23 ± 3	4.8	2.4
9c	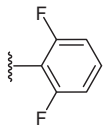	140 ± 58	73 ± 10	4.3	2.6
9d	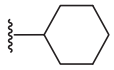	310 ± 140	183 ± 82	4.4	2.1
9e	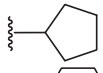	260 ± 44	270 ± 62	4.0	2.6
9f	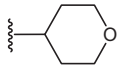	>10,000	ND	2.8	<2.2
9g	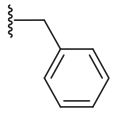	1400 ± 210	3000 ± 258	4.3	1.6

[a] IC_{50} values reflect mean +/− standard deviation of two or more determinations.
[b] Lipophilic efficiency (pIC_{50}—*c*log*P*).

Table 2
Jurkat Ca^{2+} and IL-2 secretion inhibition of selected 7-azaindole derivatives[a]

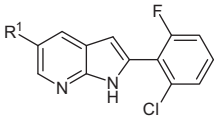

Compound	R^1	Jurkat calcium inhibition IC_{50} (nM)	Jurkat IL-2 secretion inhibition IC_{50} (nM)	*c*Log*P*	LipE[b]
14a	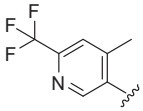	129 ± 48	120 ± 23	5.7	1.2
14b	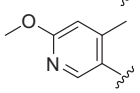	71 ± 7	40 ± 37	4.9	2.2
14c	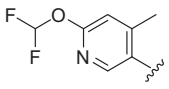	64 ± 1	150 ± 29	5.8	1.4
14d	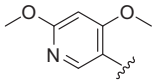	150 ± 22	68 ± 24	4.2	2.6
14e	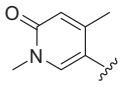	>10,000	ND	3.6	<1.4

(*continued on next page*)

Table 2 (*continued*)

Compound	R^1	Jurkat calcium inhibition IC_{50} (nM)	Jurkat IL-2 secretion inhibition IC_{50} (nM)	*c*Log*P*	LipE[b]
14f	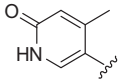	>10,000	ND	3.3	<1.7
14g	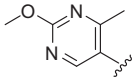	10,000	ND	3.9	1.1
14h	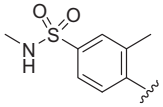	155 ± 15	180 ± 76	4.5	2.3
14i	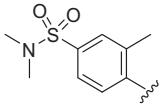	550 ± 250	119 ± 2	4.7	1.6
14j	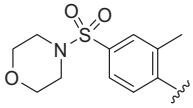	10,000	ND	4.5	0.5
14k	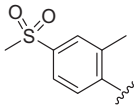	280 ± 141	290 ± 79	4.5	2.1
14l	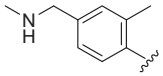	10,000	ND	5.2	0
14m	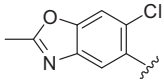	88 ± 24	117 ± 5	5.3	1.8
14n	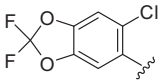	120 ± 82	56 ± 10	6.8	0.1

[a] IC_{50} values reflect mean +/− standard deviation of two or more determinations.
[b] Lipophilic efficiency (pIC_{50}—*c*log*P*).

Table 3
In vitro profile of selected derivatives

Compound	I CRAC in HEK STIM1 Orai1 overexpressing cells IC_{50} (nM) [12]	LAD2 degranulation hexosaminidase release IC_{50}* (nM)[14]	Rat whole blood IL-2 secretion inhibition IC_{50} (nM)[15]	Cytotoxicity CHO cells IC_{50} (μM)
9b	<100	372 ± 73	500	>100
14b	104	443 ± 33	1300	>100
14d	440	630 ± 34	740	>100

* IC_{50} values reflect mean +/− standard deviation of two or more determinations.

findings (data not shown). As can be seen in Table 2, disubstituted 3-pyridyl groups (**14a–d**) provided the highest potency inhibiting calcium in Jurkat cells with less than 2 fold drop between IL-2 and calcium inhibitory activity, except for compound **14c**. Compound **14b** is the only example providing IC_{50} <100 nM in the calcium and in the IL-2 assays. In an attempt to introduce more polarity, pyridones were introduced in R^1 (**14e–f**) resulting in a complete loss of potency and demonstrating that *N*-methylpyridone or hydroxy pyridine groups are not tolerated in this position of the molecule. Replacement of the pyridine ring of **14b** by a pyrimidine (**14g**) also resulted in a drop of potency similarly as when basic groups were introduced (**14l**). These results indicate that in this series, the room for SAR expansion to introduce polar solubilizing groups is very limited. Similarly, *N*-methyl (**14h**) and *N,N*-dimethyl (**14i**) 3-methylbenzenesulfonamides and sulfone **14k** provided acceptable potencies whereas the sulfonylmorpholine derivative (**14j**) was inactive. Substitution with bicyclic groups in R^1 such as 6-chlorobenzoxazole and 6-chloro-2,2-difluorobenzodioxolyl groups (**14m–n**) was also tolerated, although these molecules suffered from very high lipophilicity (*c*log*P* >5) and low solubility (<1 μg/mL).

Table 4
In vitro ADME profile of selected derivatives

Compound	Rat/human metabolism (%)[a]	PAMPA [*10^{-6} cm/s][b]
9b	<5/<5	<0.05[c]
14b	10/15	0.1
14d	10/<5	0.66

[a] Percentage of metabolism in hepatic microsomes after 30 min of incubation at 37 °C in the presence of NADPH. Compound and protein concentration were set to 5 μM and 1 mg/mL, respectively.
[b] Passive permeability through a PAMPA membrane. Compound concentration: 20 μM.
[c] The compound was not detected in the acceptor chamber.

Table 5
Wistar rat pharmacokinetic parameters of selected derivatives[a,b]

Compound	iv (1 mg/kg)				p.o (10 mg/kg)		
	$t_{1/2}$ (h)	$AUC_{(0-24)}$ (ng h/mL)	Cl (mL/min/kg)	V_{ss} (L/kg)	C_{max} (ng/mL)	$AUC_{(0-24)}$ (ng h/mL)	F (%)
14b	2.1 ± 0.2	596 ± 136	24 ± 0	4.2 ± 0.4	153 ± 57	2179 ± 985	37 ± 17
14d	8.0 ± 0.7	1824 ± 279	8 ± 1	5 ± 1	807 ± 415	11219 ± 3100	62 ± 17

[a] Mean values ± SD (n = 2).
[b] Formulation: iv: 50% PEG400 + 10% ethanol (compounds **4** and **11**) and 40% PEG300 + 10% ethanol (compound **9**); p.o.: 0.5% methylcellulose + 0.1% Tween 80.

Compounds **9b**, **14b** and **14d** were chosen to for further profiling since they exhibited the most balanced potencies in the calcium flux and IL-2 cellular assays. In terms of physicochemical properties, the lead compounds selected displayed very low solubility in water (<5 μg/mL), $c\log P$ >4 and LipE in a range of 2.2–2.4.

These compounds were profiled in further in vitro cellular assays to determine their mechanism of action through CRAC current inhibition, using an electrophysiology assay in HEK cells overexpressing STIM1/Orai1 proteins,[12] and the inhibition of mast cell degranulation through the inhibition of IgE-induced hexosaminidase release in human LAD2 cells (human mast cell line). (Table 3)[13,14] Moreover, before testing the compounds in an in vivo rat model, the inhibitory effect of the compounds on IL-2 secretion in rat whole blood was evaluated.[15] All compounds showed decreased potency in rat cells compared to that observed in human Jurkat cells in IL-2 secretion (Tables 2 and 3). Compounds were not cytotoxic up to concentrations of 100 μM, indicating that inhibitory effects observed on cellular assays are related to the mechanism of action of the compounds.

Very low metabolism was observed in both rat and human microsomes in the presence of NADPH (Table 4). PAMPA permeability results indicated lack of passive permeability for compound **9b** and limited permeability for compounds **14b** and **14d** (Table 4). Taking into consideration these results, compound **9b** was discarded for further characterization. All three compounds showed rat plasma protein binding >99.9%.

The pharmacokinetic profile of compounds **14b** and **14d** analogues was determined in rat (Table 5). Moderate clearance and volume of distribution were observed for compound **14b**. Compound **14d** had a significantly lower clearance, similar volume of distribution and increased terminal half-life. Both compounds displayed good oral exposure, with bioavailabilities higher than 35%.

To assess in vivo pharmacological activity, compound **14d** was evaluated in the ovalbumin (OVA) induced model of allergic inflammation in Brown Norway rats (Fig. 2).[16–19] Three different doses of compound **14d** (3, 10 and 30 mg/kg) were orally administered bid, 1 h before and 6.5 h after OVA challenge. Dexamethasone was included in the experiment as positive control. The anti-inflammatory potential of compound **14d** was evaluated on its ability to inhibit airway cell infiltration in bronchoalveolar lavage fluid (BALF) at the end of the experiment (24 h post OVA-challenge). A dose dependent inhibition of eosinophils in BALF of 9%, 68% and 75% respectively versus vehicle treated animals was observed. Plasma levels of compound **14** at the end of the experiment proportionally increased with dose and correlated with the inhibitory effect observed. Total plasma levels are reported since compound free levels could not be calculated due to very high plasma protein binding.

Moreover, rat whole blood IL-2 inhibition was used as surrogate pharmacodynamic marker to contextualize the efficacy observed in the rat OVA-challenged animals. This rat assay allows us to compare efficacy of the compound in target cells of the same species of the efficacy model. Although IL-2 inhibition is not linked with eosinophil infiltration inhibition, it has been reported as a practical measure of efficacy for cyclosporine A that, similar to Orai inhibitors, interferes with the NFAT pathway.[20] At the end of the experiment, plasma levels below those required for rat whole blood IL-2 IC_{50} were observed in animals showing no efficacy at inhibiting eosinophil infiltration. Animals having plasma levels >3-fold above IC_{50} for rat IL-2 inhibition showed almost 70% inhibition of eosinophils infiltration in BALF (Fig. 2).

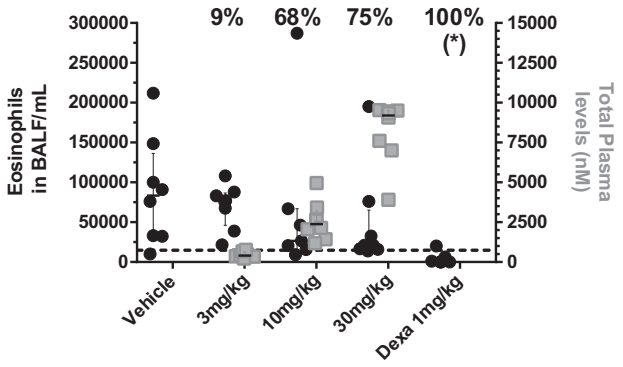

Figure 2. Dose response effect on BALF eosinophil count and total plasma levels of Compound **14d** in OVA rat model. Results are expressed as the number of eosinophils/mL in BALF (black dots), and total plasma levels (nM) (grey squares). Median values with interquartile range of the 8 animals used for each group are represented. Percentages reflect % inhibition of Eosinophils vs vehicle treated animals. Statistical analysis was done with a one way ANOVA followed by a Dunnett's test (*$p \leqslant 0.05$). Dotted line indicates plasma levels required to achieve IC_{50} of IL-2 secretion from rat whole blood cells in vitro.

In summary, we have described a series of 7-azaindole based Orai inhibitors. The initial SAR was explored, demonstrating that the nature and substitution of groups on both 2- and 5-positions of the 7-azaindole ring are essential to calcium and IL-2 inhibitory activity. Best molecules tend to be highly lipophilic, with limited room for introduction of polar groups. After further profiling of the most potent derivatives, compound **14d** was selected as a good tool for in vivo studies, as it is potent and displays good oral exposure in rat. The efficacy observed with **14d** reinforces the potential of Orai channel inhibitors for the treatment of respiratory diseases such as asthma. Further optimization with novel core rings to achieve both an improvement in Orai inhibitory activity and lower lipophilicity is essential for high quality lead compounds suitable for oral administration.

Acknowledgements

The authors acknowledge the contribution of Dr. A. Kirshenbaum and Dr. Y. Wu (NIH, Bethesda) and the US Public Health Services for providing the LAD2 cell line.

References and notes

1. Shaw, P. J.; Feske, S. *Front. Biosci.* **2012**, *4*, 2253.
2. Oh-hora, M. *Immunol. Rev.* **2009**, *231*, 210.
3. Vig, M.; Peinelt, C.; Beck, A.; Koomoa, D. L.; Rabah, D.; Koblan-Huberson, M.; Kraft, S.; Turner, H.; Fleig, A.; Penner, R.; Kinet, J.-P. *Science* **2006**, *312*, 1220.
4. Vig, M.; DeHaven, W.; Bird, G. S.; Billingsley, J. M.; Wang, H.; Rao, P. E.; Hutchings, A. B.; Jouvin, M.-H.; Putney, J. W.; Kinet, J.-P. *Nat. Immunol.* **2008**, *9*(1), 89.

5. Parekh, A. B. *Nat. Rev. Drug Disc.* **2010**, *9*, 399.
6. Feske, S. *Ann. N. Y. Acad. Sci.* **2011**, *1238*, 74.
7. Sweeney, Z. K.; Minatti, A.; Button, D. C.; Patrick, S. *ChemMedChem* **2009**, *4*, 706.
8. Rodriguez, A. L.; Koradin, C.; Dohle, W.; Knochel, P. *Angew. Chem., Int. Ed.* **2000**, *39*(14), 2488.
9. Majumdar, K. C.; Mondal, S. *Tetrahedron Lett.* **2007**, *48*, 6951.
10. *Fluorescent calcium flux assay:* Jurkat E6-1 cells were obtained from ATCC (number TIB-152TM) and maintained as ATCC recommend; in medium RPMI-1640 with 10% FBS at 37 °C and 5% CO_2. Before the assay, Jurkat cells were grown at a density of 2 million cells/mL in cell culture media (RPMI with 10% FBS) in a T-175 flask at 37 °C and 5% CO_2. The day of the assay, cells were harvested by centrifugation (5 minutes at 1500 rpm) and the pellet were suspended in assay buffer (HBSS w/o Ca^{2+} and Mg^{2+}, 20 mM Hepes and 1 mM $MgCl_2$, pH 7.4) at a density of 5 million cells/mL. Calcium depletion was initiated by the addition to the cell suspension of Thapsigargin at a final assay concentration of 10 μM. 20 μL of the cellular suspension containing Thapsigargin (100.000 cells/well) were plated in 30 μL of HBSS Ca^{2+} free, previously dispensed into 384 well plates (corning 3711), and incubated at RT for 15 min. Test compounds were diluted in DMSO 100% to get a 10^{-3} M stock solution and serial dilutions 1/3 were performed in the same solvent. Then, 0.5 μL of test compounds were added to the cells and incubated at rt for 1 h. Once this incubation was completed, 5 μL of dye solution (FLIPR Calcium 5 Express Kit, Molecular Devices), prepared as Molecular Devices recommended, were added into the assay plates followed by an extra incubation period of 1 h at room temperature. After the second incubation period, assay plates were placed into the FLIPR Tetra from Molecular Devices. Fluorescence was measured at a wavelength of 525 nm after the dye excitation at 485 nm. The initial baseline was measured during 20 s, and then 5 μL of a 25 mM calcium solution in assay buffer were added (2 mM final calcium concentration) except for basal wells, where assay buffer without calcium was added. At this time, changes in the cellular fluorescent were measured for an extra 80 s. Peak and base line were taken for the calculation of the ratio (Peak/Base Line). Total, basal and compound well ratio values were used to calculate percentage of inhibition.
11. *In vitro assay of cytokine release from T-cells:* Jurkat E6-1 cells were obtained from American Type Culture Collection (ATCC) and maintained in complete medium with 10% fetal bovine serum (FBS) at 37 °C/5% CO_2. Cells were plated in 100 μL of Dubelcco's Modified Eagle Medium (DMEM) with 1% FBS in a 96 well plate at a density of 1×10^6 cells/well and 50 μL of test compound was added. Cells were then stimulated by the addition of 50 mL of phytohemagglutinin (PHA) (final concentration 20 μg/mL) and incubated at 37 °C/5%CO_2 for 20 h. On the following day, the supernatants were collected and assayed for IL-2 levels by ELISA according to the manufacturer's protocols. The IC_{50} value was calculated as the concentration at which 50% of secreted IL-2 in vehicle is inhibited.
12. A CRAC assay optimized for compound screening was set up based on the one described by Fierro and Parekh in RBL-1 cells in (Fierro, L.; Parekh, A. B. *J. Membrane Biol.* **1999**, *168*, 9) adapted to an automated QPatch HTX platform at Evotec AG, using a BPS Bioscience generated cell line containing HuSTIM/HuOrai in HEK293 cells. Activation of ICRAC currents was achieved by passive depletion of Ca^{2+} stores by application of 10 mM EGTA in the internal buffer. Cells were held at a holding potential of 0 mV. Every 3 s, a voltage ramp from −100 to +100 mM (100 ms duration) was executed. Series resistance and Capacitance of the cells were measured just after whole-cell establishment and before execution of the voltage protocol. The QPatch system uses a 48-channel parallel amplifier for recordings of whole-cell currents. Data were filtered at 1 kHz and sampled at 5 kHz. Current amplitude was measured at −80 mV. The IC_{50} values were determined by normalizing the inhibition values obtained from independent cells (minimum $n = 3$ cells per concentration) using Synta (compound **2**) at 30 μM as positive control. All experiments were done at room temperature.
13. Kirshenbaum, A. S.; Akin, C.; Wu, Y.; Rottem, M.; Goff, J. P.; Beaven, M. A.; Rao, K.; Metcalfe, D. D. *Leuk. Res.* **2003**, *27*, 677.
14. LAD2 cells degranulation assay: the human mast cell line LAD2, established at the National Institutes of Health (NIH) was provided by Dr. Arnold Kirshenbaum through a biological materials license agreement. Cells were sensitized in its normal growth media (Complete StemPro-34 SFM, containing StemPro-34 nutrient supplement; 2 mM glutamine and 100 ng/mL SCF) by adding 100 ng/mL of biotin-labeled IgE overnight (37°, 5% CO_2) in a humidified atmosphere (90%). Sensitized LAD2 cells were washed with release buffer (137 mM NaCl, 2.7 mM KCl, 0.4 mM NaH_2PO_4, 5.6 mM glucose, 1.8 mM $CaCl_2$, 1.3 mM $MgSO_4$, 0.025% BSA) and adjusted to a density of 0.2×10^6/mL. Cells were transferred to the assay plate (10.000 cells/well) and pre-incubated with drugs for 30 min, and then activated with 125 ng/mL of streptavidin for 30 min. After the activation, supernatants were removed and transferred to another well for β-hexosaminidase determination. Cells were lyzed in 2 cycles of freeze-thaw and they were incubated for 90 min at 37 °C with 1 mM β-hexosaminidase substrate (*p*-nitrophenyl-*N*-acetyl-D-glucosamide, in citric buffer, pH 4.5). Reaction was stopped with 0.4 M glycine solution (pH 10.0) and absorbance was read at 405 nm.
15. Rat whole blood cells were diluted 1:4 in RPMI cell culture medium and stimulated by Concanavalin A (ConA) at 62.5 μg/mL in 96-well plates with increasing concentrations of the test compounds for 24 h. After that period, and upon centrifugation supernatants were transferred to a new plate and IL-2 detection was performed using Rat IL-2 DuoSet (DY502 from R&D) following the manufacturer instructions. A standard rat IL-2 curve was included for quantification purposes.
16. Brown Norway rats (200-250 g) were sensitized with Ovalbumin/Aluminium (OVA/Alum) i.p. (days 0, 14 and 21) and challenged with OVA aerosol on day 28 (Devilbiss).Compound 14d was formulated in D-alpha-tocopheryl polyethylene glycol 1000 succinate (TPGS) 11.7%, PEG-400 40%, propylen glycol 15%, water 33.3% and was dosed at 3, 10 and 30 mg/kg orally one hour prior to OVA challenge and 6.5 h after challenge (to sustain compound levels). Eight animals were included per treatment group. 24 h after OVA challenge, bronchoalveolar lavage fluid (BALF) was collected to determine cell counts (Sysmex). Plasma samples were analyzed by UPLC-MS after protein precipitation.
17. Garlisi, C. G.; Falcone, A.; Hey, J. A.; Paster, T. M.; Fernandez, X.; Rizzo, C. A.; Minnicozzi, M.; Jones, M.; Billah, M. M.; Egan, R. W.; Umland, S. P. *Am. J. Respir. Cell Mol. Biol.* **1997**, *17*, 642.
18. Underwood, S. L.; Raeburn, D.; Lawrence, C.; Foster, M.; Webber, S.; Karlsson, J. A. *Br. J. Pharmacol.* **1997**, *122*(3), 439.
19. Underwood, S. L.; Haddad, E.-B.; Birrell, M. A.; McCluskie, K.; Pecoraro, M.; Dabrowski, D.; Webber, S. E.; Foster, M. L.; Belvisi, M. G. *Br. J. Pharmacol.* **2002**, *137*, 263.
20. Stein, C. M.; Murray, J. J.; Wood, A. J. *J. Clin. Chem.* **1999**, *45*(9), 1477.